On the Anticorrelation between Duration and Redshift in Gamma-Ray Bursts

Nicole Lloyd-Ronning[1,2] , Jarrett Johnson[1] , Roseanne M. Cheng[1] , Ken Luu[1,3], Phoebe Upton Sanderbeck[1],
Lailani Kenoly[1], and Celia Toral[1,4]
[1] Los Alamos National Lab, Los Alamos, NM 87545, USA
[2] Department of Math, Engineering, & Science, University of New Mexico, 4000 University Drive, Los Alamos, NM 87544, USA
[3] San Francisco State University, San Francisco, CA 94132, USA
[4] Cornell University, Ithaca, NY 14850, USA

Abstract

For gamma-ray bursts (GRBs) with durations greater than two seconds (so-called long GRBs), the *intrinsic* prompt gamma-ray emission appears, on average, to last longer for bursts at lower redshifts. We explore the nature of this duration–redshift anticorrelation, describing systems and conditions in which this cosmological evolution could arise. In particular, we explore its dependence on the metallicity of a massive star progenitor, because we can securely count on the average stellar metallicity to increase with decreasing redshift. Although stars with higher metallicity/lower redshift lose mass and angular momentum through line-driven winds, in some cases these stars are able to form more extended accretion disks when they collapse, potentially leading to longer-duration GRBs. We also examine how this duration–redshift trend may show up in interacting binary models composed of a massive star and compact object companion, recently suggested to be the progenitors of radio-bright GRBs. Under certain conditions, mass loss and equation-of-state effects from massive stars with higher metallicity and lower redshift can decrease the binary separation. This can then lead to spin-up of the massive star and allow for a longer-duration GRB upon the massive star's collapse. Finally, the duration–redshift trend may also be supported by a relatively larger population of small-separation binaries born in situ at low redshift.

Unified Astronomy Thesaurus concepts: Gamma-ray bursts (629); Close binary stars (254); Massive stars (732)

1. Introduction

There is strong evidence that most long gamma-ray bursts (GRBs), those with prompt gamma-ray durations of more than about two seconds, are associated with the collapse of a massive star. Observationally, there exist definitive associations of Type Ibc supernovae with long GRBs (Galama et al. 1998; Hjorth et al. 2003; Hjorth & Bloom 2012). Theoretically, such progenitors provide the necessary energy reservoir over the relevant timescales (Woosley 1993; MacFadyen & Woosley 1999; Woosley & MacFadyen 1999; Woosley & Bloom 2006; Woosley & Heger 2006; Kumar et al. 2008a).

However, the details of GRB progenitors are still far from resolved. The central engine is believed to be a highly spinning black hole–disk system[5] that launches a very relativistic jet. Internal dissipation processes in the jet produce the prompt gamma-ray emission, while the subsequent afterglow (emitted across the electromagnetic spectrum) results from the jet front's interaction with the external medium. But which massive stars are capable of producing such powerful jets and why (i.e., what are the key parameters that allow certain massive stars to create a GRB)? One key approach to answering this question is to examine the evolution of GRB properties over cosmic time, and attempt to understand that evolution in the context of particular progenitor systems. For example, the evolution of GRB jet opening angle with redshift (Lü et al 2012; Laskar

et al. 2014, 2018a, 2018b; Lloyd-Ronning et al. 2019b; Chakraborty et al. 2023) connects GRBs with massive stars in a unique way. Lloyd-Ronning et al. (2020) showed that the smaller jet opening angles at higher redshifts can be quantitatively explained by a massive star's envelope collimating the jet, and this is consistent with evolving models for the initial mass function reported in the literature (e.g., Davé 2008).

In this vein, we examine the nature of the evolution of GRB prompt duration over redshift. Taking care to account for selection effects, Lloyd-Ronning et al. (2019a) found a statistically significant anticorrelation between intrinsic duration (that is, duration corrected for cosmological time dilation) and redshift in a sample of 376 long GRBs. Lloyd-Ronning et al. (2019b) confirmed this in a subsample of radio-bright GRBs with isotropic equivalent energies above 10^{52} erg. Recently Chakraborty et al. (2023) further confirmed this trend, employing different techniques to account for data selection effects that could have artificially produced this intrinsic duration–redshift anticorrelation.

How might this cosmological evolution of GRB prompt duration arise? We might, at first glance, expect that it is the *lower-metallicity* stars (at high redshift) that would produce longer-duration GRBs; higher-metallicity massive stars (at lower redshifts) lose more mass and angular momentum (through line-driven winds) than lower-metallicity stars (e.g., Puls et al. 2008). Under the assumption that systems with higher angular momentum are capable of producing longer-duration GRBs (Proga & Begelman 2003; Janiuk & Proga 2008; Lloyd-Ronning 2022), we would then naively expect to see, on average, longer-duration GRBs at higher redshifts. That the *opposite* trend is seen in the data suggests this expectation warrants closer examination.

---

[5] There are also viable models with a neutron star as the central engine (e.g., Lin et al. 2020).

In this paper, we qualitatively consider different progenitor scenarios for long GRBs in which this unexpected correlation could arise, focusing particularly on the role metallicity plays in determining the properties of these systems and their post-collapse GRB jets. We first examine the presence of this correlation in the context of the collapse of a single star. We then consider progenitor systems with a massive star collapsing in an interacting binary system, and examine whether the evolution of binary properties with redshift can account for the observed duration–redshift anticorrelation. Our paper is organized as follows. In Section 2, we discuss the data and summarize the evidence for this correlation. Then, in Section 3, we describe how single-star progenitors might produce this duration–redshift trend. Recognizing the strong assumptions necessary in single-star progenitor models for long GRBs, Section 4 is devoted to exploring how this trend may show up in binary progenitor models for long GRBs. In Section 5, we present discussion and summarize our conclusions.

2. Observed Correlation

Lloyd-Ronning et al. (2019a) looked at a sample of 376 long GRBs with measured redshifts, and corrected the durations for cosmological time dilation to get the intrinsic duration: $T_{int} = T_{90}/(1+z)$, where T_{90} is the measured duration of 90% of the photon counts and z is redshift. They found T_{int} appears on average to decrease with redshift—that is, gamma-ray bursts' intrinsic prompt durations are on average longer at lower redshifts. It is important to consider whether this correlation has a true physical origin or is a result of observational selection effects. For example, *for a given luminosity*, a high-redshift GRB will have a lower flux and some of the emitted flux could in principle be "shifted" beneath the detector noise, making the GRB time profile appear shorter than it really is (i.e., with an apparently shorter duration; a recent example of this effect in the context of ultralong-duration GRBs is found in Huang et al. 2022). However, GRBs are *not* standard candles in their luminosities and in fact have much scatter in this variable; in other words, a higher-redshift GRB does *not* necessarily imply a lower flux, and therefore this effect is substantially mitigated (Lee et al. 2000). In fact, many studies have suggested GRBs are brighter at high redshifts, which would further mitigate (if not eliminate) this selection effect. Nonetheless, taking a conservative approach to account for such biases using non-parametric methods of Lynden-Bell (1971) and Efron & Petrosian (1992), Lloyd-Ronning et al. (2019a) found a statistically significant ($\sim 4\sigma$, p-value of 10^{-4}, where the null hypothesis is no redshift evolution) anti-correlation between intrinsic duration and redshift: $T_{int} \propto (1+z)^{-0.8 \pm 0.2}$. This correlation is shown in Figure 1, with data points binned (every 20 GRBs) for clarity (large blue dots).

This correlation shows up even more prominently in certain subsamples of long GRBs. Lloyd-Ronning et al. (2019b) found this correlation exists with even higher statistical significance in radio-bright GRBs (that is, those GRBs for which radio follow-up was attempted and an afterglow was detected; note that in their analysis, they examined only those GRBs with isotropic equivalent energies above 10^{52} erg). In their radio-bright subsample consisting of 79 GRBs, they found a $\sim 5\sigma$ correlation (p-value $\sim 5 \times 10^{-5}$), with $T_{int} \propto (1+z)^{-1.4 \pm 0.3}$. Recently, Chakraborty et al. (2023) reanalyzed this correlation with an updated, larger sample of radio-bright and radio-dark

GRBs, using a variety of approaches to account for selection effects. Even with fairly stringent and conservative assumptions about the biases, they found the correlation still exists, with $T_{int} \propto (1+z)^{-1.3 \pm 0.3}$ (p-value of 10^{-6}) for the radio-bright GRB sample and $T_{int} \propto (1+z)^{-1.2 \pm 0.4}$ (p-value of 10^{-3}) for the radio-dark sample. The unbinned radio-bright (magenta) and radio-dark (lime) duration–redshift data are shown in Figure 1.

The presence of this correlation, if indeed physical, can offer important clues to the progenitor systems of long GRBs. Because the duration of a GRB (in the context of a black hole–disk central engine) is roughly proportional to the amount of mass in the disk divided by its accretion rate[6] (i.e., $T_{int} \sim M/\dot{M}$), longer-duration GRBs at lower redshifts imply these systems have more massive accretion disks, lower accretion rates, or both. Of course, extrapolating from the final state of the progenitor star (or stars) to the black hole–disk system that produces the GRB jet is not straightforward (Halevi et al. 2022). However, we might expect general trends to hold —for example, a more extended massive star and/or one with an overall higher angular momentum reservoir may be able to produce a longer-lived jet upon collapse, leading to a longer-duration GRB (see the recent arguments in Lloyd-Ronning 2022).

3. Single-star Models

A single massive star collapsing to a black hole–disk central engine—the so-called collapsar model (Woosley 1993; MacFadyen & Woosley 1999; Woosley & MacFadyen 1999)—has for some time been the canonical model for long gamma-ray bursts. As long as the star can retain enough angular momentum to launch a jet (with enough momentum to punch through any existing stellar envelope), this progenitor provides the necessary overall energy budget to power a long GRB. Several types of massive stars have been suggested as viable progenitors of GRBs, including red supergiants (RSGs; Nakauchi et al. 2012; Quataert & Kasen 2012; Wu et al. 2013; Liu et al. 2018), blue supergiants (BSGs; Perna et al. 2018), and Wolf–Rayet (WR) stars (Meynet & Maeder 2005; Georgy et al. 2009, 2012). In particular, WR stars have been suggested as viable progenitors because of their stripped hydrogen envelopes—the stripped envelope not only makes it more viable for the jet to break free from the star but is also consistent with the lack of hydrogen lines in the spectra of supernovae associated with some GRBs.[7] However, Suwa & Ioka (2011), Nagakura et al. (2012), Perna et al. (2018), and others have shown that it is indeed possible for a jet to break out from RSG and BSG progenitors. Therefore, our arguments are applied in a fairly general way, as the details of the progenitor stars able to produce a GRB are still up for debate.

We consider how the duration–redshift anticorrelation might arise in isolated stellar systems, particularly as a function of metallicity (again, because this securely increases with decreasing redshift). As mentioned in the introduction, we might naively expect that, because higher-metallicity stars lose more mass and angular momentum than lower-metallicity stars (Woosley & Heger 2006), they would produce on average *shorter*-duration GRBs, opposite to the trend we see in the data

---

[6] This rough proportionality is simply a dimensional analysis argument, but see Janiuk & Proga (2008) and Kumar et al. (2008b) for more detailed arguments.

[7] We also note the result by Han et al. (2010), who observed populations of WR stars in the host galaxies of some GRBs.
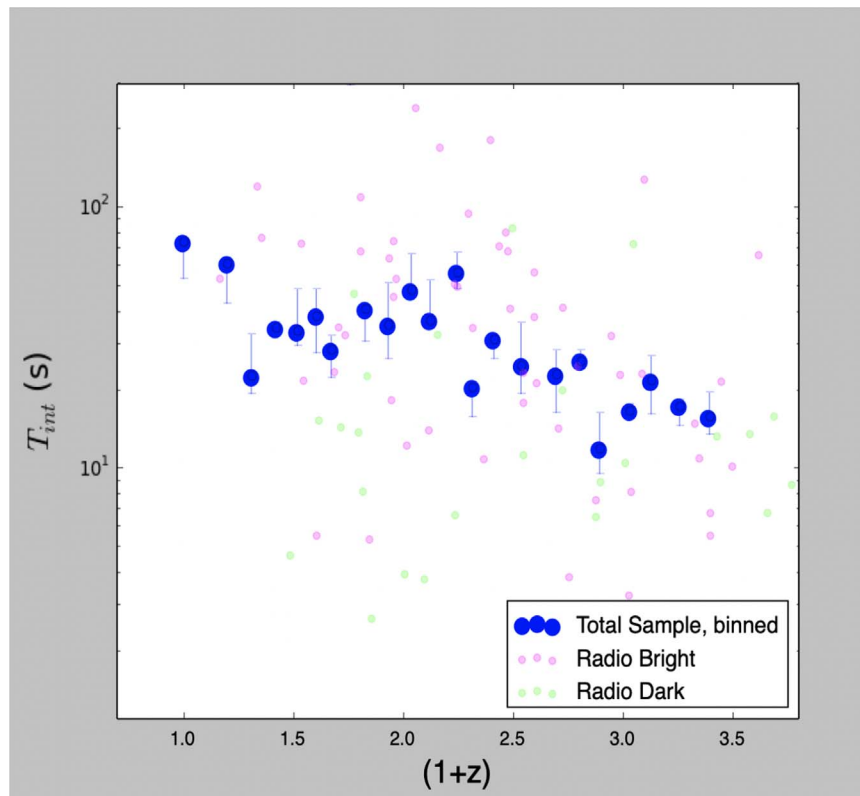
Figure 1. Intrinsic gamma-ray duration (corrected for cosmological time dilation) as a function of redshift for 376 GRBs with redshift measurements. The data are from Lloyd-Ronning et al. (2019b) and binned every 20 GRBs, for clarity. We also show the unbinned data, divided into radio-bright (magenta) and radio-dark (lime) subsamples. The on-average shorter prompt duration of the radio-dark sample is evident. Detailed explanations of the statistical analysis of this correlation for the whole sample as well as radio-bright and -dark subsamples are found in Lloyd-Ronning et al. (2019a, 2019b) and Chakraborty et al. (2023).

(although see Maeder 2002, who shows that anisotropic—specifically, polar-enhanced—mass loss leads to an *increase* in stellar rotational velocity; and indeed Olivier et al. 2022 show observations of an 80 $M_\odot$ star undergoing such bipolar mass loss).

However, higher-metallicity stars are also, on average, less dense/have larger radii than low-metallicity stars (Maeder & Meynet 2001; Georgy et al. 2013). This is established observationally in dwarf stars (Houdebine 2008).[8] In the case of high-mass stars, the observations are more tenuous (although see Harada et al. 2019; Gieser et al. 2021). Though secure measurements of metallicity and radius are more difficult to come by, Farrell et al. (2022) have shown through a number of detailed numerical simulations of massive star evolution that lower-metallicity stars are indeed more compact due to lower opacity in the stellar envelope as well as lower CNO abundances in the burning regions of the star. Sanyal et al. (2017) explore the metallicity dependence of envelope inflation in massive stars and find, consistent with expectations, that, for a given mass, low-metallicity stars haven smaller radii than high-metallicity stars (see their Figures 2 and 11).[9] Xin et al. (2022) make an estimate of the dependence of a 15 $M_\odot$ star's radius on metallicity, modeling the star with the stellar evolution code MESA, and also see a significant increase in the stellar radius with metallicity, over the range of metallicities they consider (Z between 0.0001 and 0.03). Tout et al. (1996) and Maccarone et al. (2004) found that the radius of a star is proportional to metallicity roughly to the 1/8 power.

What are the implications of this for single-star progenitors of long GRBs (and, in particular, for the lifetime of the jets they create and therefore the timescale of the prompt emission)? We can get a handle on the duration of the GRB jet by estimating the interval over which stellar material feeds the central engine upon collapse. In other words, the freefall time, given by $t_{ff} \approx 4298$ s $\times (R^3/M)^{1/2}$, can be used as a rough estimate for the lifetime of the disk that will form around the central black hole. As long as there is sufficient angular momentum to launch the GRB jet, simply the difference in the stellar radius at different metallicities can therefore qualitatively explain the trend we see in the data. We represent this in Figure 2, which shows the freefall time as a function of stellar radius, for stars of different masses. Imposed on the plot are a set of stellar evolution simulations we ran with the 1D stellar evolution code MESA (Paxton et al. 2011, 2013, 2015, 2018, 2019; Paxton 2021).[10] The models on the plot show stars of 25 solar masses (purple symbols) and 40 solar masses (lime symbols) at different metallicities ranging from $Z = 0.0001$ to $Z = 0.1$, where Z is the mass fraction of "heavy" elements (heavier than helium) relative to the total mass of the gas. Not shown on the plot are a suite of 60 solar-mass models that show similar trends to those we describe below. The MESA equation of state

---

[8] Although see Boyajian et al. (2012), who do not find a strong dependence on metallicity for many physical properties of *low-mass* stars.

[9] We note the results of Chun et al. (2018), whose simulations of RSGs with 1D stellar evolution codes show that the final radii of these stars' hydrogen envelopes are largely independent of metallicity (over the range $Z = 0.004–0.04$). However, GRB models (and observations of their coincident Type Ic supernovae) generally require a stripped hydrogen envelope, and so these models may not apply to our study.
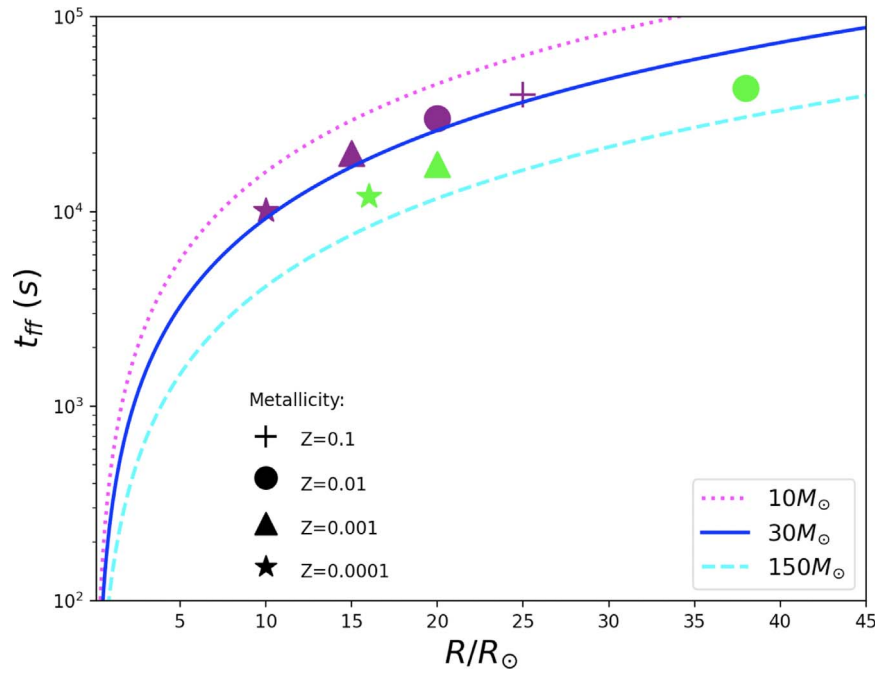
[10] We use release r21.12.1.

Figure 2. Freefall time as a function of stellar radius for stars of different masses. The plotted symbols show the radius of an evolved 25 $M_\odot$ star (purple) and a 40 $M_\odot$ star (lime) for different metallicities (denoted by different symbols indicated in the lower left of the plot), using the MESA stellar evolution code. As expected stars of higher metallicity have larger radii near the end of their evolution. We find the radius depends on metallicity roughly as $R \propto Z^{1/8}$ for the 25 $M_\odot$ star, consistent with Tout et al. (1996) and Maccarone et al. (2004). The relationship holds for the 40 $M_\odot$ star at lower metallicities but has a stronger dependence at higher metallicities. We note that metallicity, as we have defined it here, is the fraction of elements heavier than helium; solar metallicity in these units is $Z \approx 0.019$.

(EOS) is a blend of the OPAL (Rogers & Nayfonov 2002), SCVH (Saumon et al. 1995), FreeEOS (Irwin 2004), HELM (Timmes & Swesty 2000), PC (Potekhin & Chabrier 2010), and Skye (Jermyn et al. 2021) EOSs. Radiative opacities are primarily from OPAL (Iglesias & Rogers 1993, 1996), with low-temperature data from Ferguson et al. (2005) and the high-temperature, Compton-scattering-dominated regime by Poutanen (2017). Electron conduction opacities are from Cassisi et al. (2007) and Blouin et al. (2020). Nuclear reaction rates are from JINA REACLIB (Cyburt et al. 2010), NACRE (Angulo et al. 1999), and additional tabulated weak reaction rates (Fuller et al. 1985; Oda et al. 1994; Langanke & Martínez-Pinedo 2000). Screening is included via the prescription of Chugunov et al. (2007). Starting with the pre-main-sequence model option in MESA, we evolve the stars until the fraction of helium in the core falls below 10^{-3}, and have done so with a range of spatial and temporal resolution parameters until convergence. As expected, and consistent with the results quoted in the previous paragraph, there is a clear trend of larger radius for higher metallicity.

We note that Table 2 of Woosley & Heger (2006) also shows a general trend among all of their models of a smaller iron core mass with increasing metallicity. This means that not only is the stellar radius more extended in higher-metallicity stars but they can contain more mass; there is therefore a larger reservoir of fuel to feed the black hole and sustain the jet for a longer time.

Metallicity has also been shown to slow accretion rate (Wei & Liu 2022). The accretion rate (due to fallback) is estimated as $\dot{M} \sim dM_r/dt_{\rm ff}$, where M_r is the mass contained in a radius r. Related to our arguments above, a higher-metallicity (more extended, less dense) star will have a longer fallback accretion timescale and therefore lower accretion rate (see also Equation (11) of Suwa & Ioka 2011). Additionally, higher stellar opacity

leads to larger radiation pressure that can stall accretion (Fukushima et al. 2018). Toyouchi et al. (2019) show how metallicity decreases the accretion rate even in the case of super-Eddington accretors.[11]

The arguments above suggest that higher-metallicity isolated stars can in principle produce longer-duration GRBs provided these systems have enough angular momentum to launch a jet. This, of course, is a strong assumption (see, e.g., Proga & Begelman 2003 and Janiuk & Proga 2008 for discussions on the difficulty of single stars retaining enough angular momentum upon collapse to produce a long-duration GRB), and has led to some authors considering massive stars collapsing in an interacting binary system as a way to increase or sustain the angular momentum of the massive star upon collapse. We now discuss this correlation in the context of that scenario.

4. Interacting Binary Star Models

Recently, Lloyd-Ronning (2022) examined the particular case of a massive star collapsing in a tidally locked system with a black hole companion.[12] Observationally, we know such systems exist as high-mass X-ray binaries (HMXBs). As discussed in Tauris & van den Heuvel (2006), these systems (as observed in our own Galaxy) have massive star companions

---

[11] However, GRBs are known to be extremely super-Eddington accretors (more than 10–15 orders of magnitude above the Eddington rate), and it is not clear exactly how strong an effect metallicity will have in this case.

[12] Their work was motivated by the apparent dichotomy between radio-bright and -dark GRBs—as discussed above, several works have shown that the radio-bright population has on average significantly longer prompt gamma-ray durations and isotropic equivalent energy compared to the radio-dark population. In her model, Lloyd-Ronning (2022) shows these systems can explain the longer-duration gamma-ray emission, higher isotropic energy, and the presence of radio emission in the radio-bright subpopulation of GRBs.

greater than 20 solar masses and with radii of 10–20 solar radii. They appear to almost fill their critical Roche lobes. Their orbital periods are <10 days and they have low eccentricity. Motivated by this, we consider how the anticorrelation between T_{int} and $(1 + z)$ may arise in systems that consist of a massive star in a tidally locked binary with a black hole companion.

All of the points made in the previous section relevant to single-star models will also apply to the massive star in our binary. However, here we consider how the interaction of the massive star with its companion affects the state of the star at the end of its life. In particular, we consider the angular momentum of the massive star right before collapse and relate this to the duration of the GRB jet. We then examine how this depends on the metallicity of the system, in order to understand how these systems (and their GRB durations) might evolve over redshift.

The net angular momentum (denoted by J) in a binary system is given by

$$J_{\mathrm{binary}} = J_{\mathrm{orb}} + J_* + J_{\mathrm{BH}} = \left[\frac{aG(M_*M_{\mathrm{BH}})^2}{M_* + M_{\mathrm{BH}}} \right]^{1/2}$$
$$+ I_*\omega_* + I_{\mathrm{BH}}\omega_{\mathrm{BH}} \qquad (1)$$

where a is the binary separation, G is the gravitational constant, M_* is the mass of the massive star, M_{BH} is the mass of the black hole, ω_* is the rotational rate of the massive star, ω_{BH} is the rotational rate of the black hole, I_* is the moment of inertia of the massive star, and I_{BH} is the moment of inertia of the black hole. We approximate the moments of inertia of each object as $I \approx \alpha MR^2$, where α is a constant of order unity and R is the radius of the spinning object (massive star or black hole).

If we assume our system is tidally locked (with zero eccentricity),[13] the orbital frequency $\omega_{\mathrm{orbit}} = \omega_* = \omega_{\mathrm{BH}} = \sqrt{GM_{\mathrm{tot}}/a^3}$, where $M_{\mathrm{tot}} = M_{\mathrm{BH}} + M_*$. In this special case the total angular momentum in the system can be written as

$$J_{\mathrm{binary}} = \left[\frac{aG(M_*M_{\mathrm{BH}})^2}{M_* + M_{\mathrm{BH}}} \right]^{1/2} + \left[\frac{G(M_* + M_{\mathrm{BH}})}{a^3} \right]^{1/2}$$
$$\times [\alpha_{\mathrm{BH}}M_{\mathrm{BH}}R_{\mathrm{BH}}^2 + \alpha_*M_*R_*^2]. \qquad (2)$$

Again, here our goal is to consider how the angular momentum of the massive star (inextricably linked to the intrinsic duration of the prompt GRB) depends on the parameters of this interacting binary system—particularly metallicity—and how this could lead to the evolution of GRB prompt duration as a function of redshift.

Just as in the single-star case, a higher-metallicity massive star in such a system will lose more mass due to line-driven

winds than one of low metallicity. This nonconservative mass loss can lead to the binary widening (Broekgaarden et al. 2022), and decrease the binary interaction (lessening the potential spin-up of the massive star).[14] Therefore, as in the single-star case, we might at first glance expect higher-metallicity systems to have lower angular momentum and therefore shorter-duration GRBs. However, this ignores a number of other subtle factors that can decrease the binary separation and lead to spin-up of the massive star. For example, a higher-metallicity massive star in a binary system may also be more likely to undergo conservative mass loss through Roche lobe overflow, while these stars are less compact, and this can serve to tighten our binary. Drag forces by ambient gas can also play an important role and lead to a decrease in the binary separation. We now discuss scenarios in which (ultimately metallicity-dependent) changes in mass and radius affect the binary system and play a role in the duration of a GRB.

In short, higher metallicity serves to increase both conservative and nonconservative mass loss (of which the former will lessen the binary separation and the latter will increase it), and there is a competition at play between these two effects. Additionally, higher-metallicity systems can play a complicated role in other effects such as anisotropic mass loss and drag forces (both of which decrease our binary separation). Below we delve into this issue in more detail as we attempt to understand the role of metallicity in the evolution of binary separation.

4.1. Evolution of Binary Separation

How the separation between two stars in a binary system evolves over the lifetime of each star is a complicated problem with many possible outcomes, depending on the physical properties of the stars, the initial binary separation, the nature of each star's mass loss, and the system's environment.

It is crucial to point out that we observe a number of HMXB systems (similar to the systems we consider here) that are indeed undergoing a decrease in their orbital separation—for example, Cen X-3 (Kelley et al. 1983), SMC X-1 (Levine et al. 1993), LMC X-4 (Levine et al. 2000), and seven additional HMXBs (Falanga et al. 2015), all with orbital decay timescales of the order of about a half a million years (see Table 3 of Falanga et al. 2015).

For the idealized case of two pointlike masses, we can write the normalized change in binary separation as (Postnov & Yungelson 2014)

$$\frac{\dot{a}}{a} = -2\frac{\dot{M}_*}{M_*}\left[1 + (\alpha - 1)\frac{M_*}{M_{\mathrm{BH}}} - \frac{\alpha M_*}{2M_{\mathrm{tot}}} \right] + 2\frac{\dot{J}_{\mathrm{orb}}}{J_{\mathrm{orb}}} \qquad (3)$$

where $\dot{M}_* < 0$ (i.e., the star is losing mass). Note that $\dot{M}_*$ and $\dot{J}_{\mathrm{orb}}$ are not independent variables. The parameter α is the fraction of the mass lost from M_* that *leaves* the system. That is, for $\alpha = 0$, all the mass lost from our star stays in the binary system; for $\alpha = 1$, all of it leaves the binary system.

In the case of conservative mass transfer ($\alpha = 0$ and $\dot{J}_{\mathrm{orb}} = 0$), when all of the massive star's lost mass is deposited onto the black hole, the ratio of final to initial binary separation

---

[13] This is an arguably justifiable assumption; the tidal locking timescale is given by (Gladman et al. 1996)

$$t_{\mathrm{lock}} \approx 10^3 \text{ yr } (r/10^{12} \text{ cm})^6 (\rho_{\mathrm{star}}/10^3 \text{ g cm}^{-3})(\omega_o/10^{-5} \text{ s}^{-1})$$
$$\times (Q/100)(M_{\mathrm{BH}}/10 \ M_\odot)^2(k_2/0.1),$$

where ρ_{star} is the average density of the star, ω_o is its initial rotational velocity, Q is the so-called dissipation function of the star, and k_2 is the tidal Love number. Quantities such as Q and k_2 are highly unknown (Gladman et al. 1996) and usually taken to be around ∼100 and of order unity, respectively.

[14] We note again that mass loss could be anisotropic as discussed in Maeder (2002), which can lead to spin-up of the massive star. As mentioned in the previous section, such anisotropic mass loss is observed in a massive star in an interacting binary system closely related to the ones we consider here (Olivier et al. 2022).

is given by (Postnov & Yungelson 2014)

$$\frac{a_f}{a_i} = \left(\frac{M_{\mathrm{BH},i} M_{*,i}}{M_{\mathrm{BH},f} M_{*,f}} \right)^2 \qquad (4)$$

where i and f denote initial and final states, respectively. For a massive star that is more massive than the black hole companion, as we reasonably assume is the case here (Heger et al. 2003; Ramachandran 2022),[15] the binary orbit will shrink as M_* transfers mass to the black hole. As a result, the system's angular frequency ω increases, and (because the system is tidally locked) the massive star's rotation rate increases. As mentioned above, this provides a larger angular momentum reservoir, which can lead to a longer-duration GRB (Lloyd-Ronning 2022). In such a scenario, more mass loss would therefore lead to a longer-duration GRB. However, conservative mass loss applies primarily in the case of Roche lobe overfill. In general, mass loss from winds (either isotropic mass loss or pole-dominated anisotropic mass loss) is *not* conservative and some mass will escape the system.

In the case when all of the mass directly leaves the system (perfect nonconservative mass loss with $\alpha = 1$ or the so-called Jeans mode), the binary separation will increase in order to conserve angular momentum. However, there are situations of nonconservative mass loss that lead to reduced orbital separation. For example, in the case when accretion from the massive star onto the black hole exceeds the Eddington limit, matter can be expelled from the system by radiation pressure. In this case, angular momentum is depleted from the accretor and the orbital separation can exponentially shrink with mass loss (see Equation (43) of Postnov & Yungelson 2014):

$$\frac{a_f}{a_i} = \left(\frac{M_{\mathrm{BH},i}}{M_{\mathrm{BH},f}} \right) \left(\frac{M_{*,i}}{M_{*,f}} \right) \exp\left(-2 \frac{M_{*,i} - M_{*,f}}{M_{\mathrm{BH}}} \right). \qquad (5)$$

Hence, in a realistic system there are a number competing effects when we consider the role of metallicity-driven mass loss as it affects our binary system and ultimately the spin of the massive star.

Finally, we note that drag forces can also have an important effect on the system's evolution. Schröder et al. (2021) showed that, under the assumption of nonspinning stars, line-driven winds can either tighten or widen the binary depending on the mass ratio of the binary as well as on the ratio of the wind velocity to orbital velocity. They found that for slower winds (relative to the orbital velocity) and higher-mass companions, drag forces serve to shrink the binary separation (see their Figure 1). Interestingly, Falanga et al. (2015) report inferred wind speeds for the massive stars in 10 HMXBs of the order of 1000 km s^{-1} (see their Table 9). Meanwhile, the orbital velocities for our closely separated, tightly bound binaries are about an order of magnitude higher than this, satisfying the

necessary condition on the velocity ratio that leads to a decrease in binary separation.[16]

4.1.1. The Effect of Stellar Expansion

As mentioned in the previous section on single-star progenitors, higher-metallicity stars are more extended in radius. A more extended star can have a higher moment of inertia and therefore—for a given rotation rate—higher angular momentum. Therefore, as the star expands, the binary separation will decrease (in order to conserve angular momentum in the system as a whole). Levine et al. (1993, 2000) derive an expression for this change in orbital period P_{orb} as a function of the change in the moment of inertia of an expanding star:

$$\frac{\dot{P}}{P} = \frac{3\dot{a}}{2a} \approx \frac{\omega_{\mathrm{BH}} d \ln I_* / dt}{\omega (\mu a^2 / 3 I_* - 1)} \qquad (6)$$

where μ is the binary reduced mass.[17] This equation only accounts for radial expansion and assumes the mass stays constant. As mass is lost, the moment of inertia will decrease accordingly. However, if the normalized mass lost to winds is less than twice the normalized change in radius due to stellar expansion,

$$\Delta M / M < 2 \Delta R / R, \qquad (7)$$

then the star's expansion will "win" and serve to decrease the separation in our binary system. Again, in our tidally locked model, this leads to spin-up of our massive star.

The rate of mass loss due to line-driven winds is a complicated and unresolved problem. However, it is reasonable to expect the condition in Equation (7) holds, while stellar winds are often weaker than simple models predict. We refer the reader to the review by Smith (2014) for an in-depth look at this issue, and also Fullerton et al. (2006), who showed, observationally, that stellar models tend to overestimate mass loss due to winds by a factor of 10 or more, when realistic conditions (such as clumping) are not considered.

In short, there is a complicated interplay of many different factors related to changes in mass and stellar radius that can serve to either increase or decrease the binary separation. In the next section, we focus on the consequences of the cases in which binary separation decreases with (metallicity-driven) mass loss and relate this to the observed anticorrelation between GRB duration and redshift.

4.2. Reproducing the Anticorrelation

As discussed above, there exist various scenarios in which the binary separation will decrease for systems consisting of a massive star with a compact object companion. In our model, where the tidal locking timescale is relatively short compared to other timescales in the system (e.g., orbital decay time, lifetime of star), the decreased separation will lead to a more rapidly spinning massive star, which is capable of producing a longer-duration gamma-ray burst. We would like to understand

---

[15] We note that if the binary system was born in situ (rather than through dynamical capture), the black hole companion must be the result of the more massive of the two original stars in the binary. However, we assume the death of the first massive star left a remnant black hole that is less massive than the second massive star (the one we consider here as the GRB progenitor).

[16] In our systems, we are typically considering a massive star with a compact object companion whose mass is expected to be less than that of the massive star and so—although drag forces may play an important role in the evolution of binary separation—the Schröder et al. (2021) calculations may not apply to our models.

[17] Recall, in our scenario, $\omega_{\mathrm{BH}} \sim \omega$ (the orbital angular frequency), which simplifies the equation.

how the increase in average metallicity over cosmic time may affect properties of interacting binary systems, and how this might lead to the observed anticorrelation between prompt GRB and redshift.

We parameterize the binary system's decrease in separation as a function of the donor star's mass loss as follows:

$$\frac{a_f}{a_i} \propto \left(\frac{\Delta M_*}{M_*} \right)^{-\beta} \tag{8}$$

where $\beta > 0$ parameterizes the extent to which the orbit shrinks as a function of mass loss. Once again, when considering how Equation (8) describes separation as a function of cosmic time, we will consider the variables' dependences on metallicity.

As discussed in the previous section, mass loss from both winds and Roche lobe overflow will depend on metallicity. Several groups have parameterized the former relationship, showing that mass loss from winds is $\Delta M \propto Z^{1/2}$ (Vink et al. 2001; Woosley & Heger 2006; Yoon et al. 2006). Mass loss due to Roche lobe overflow is not as well parameterized and depends on a number of factors in the system; however, given that the radius of the star depends on metallicity roughly to the 1/8 power as discussed above (Tout et al. 1996; Maccarone et al. 2004), then the dependence of mass loss on metallicity due to Roche lobe overflow can be estimated as $\Delta M \propto Z^{2/8}$ to $Z^{3/8}$ (the former considers only surface mass loss). Substituting these relationships into Equation (8), we find then that $a_f/a_i \propto Z^{-\beta/2}$ to $Z^{-\beta/4}$.

Because the angular momentum of the massive star is inversely proportional to binary separation under the tidal locking assumptions of our model, $J_* \propto a_f^{-3/2}$, we find a relationship between the star's angular momentum and its metallicity (in this special case of an interacting binary):

$$J_* \propto Z^{3\beta/4}. \tag{9}$$

Equation (9) is considering the angular momentum of the star as it depends on binary separation in a tidally locked system. At the same time, the star's winds will carry away angular momentum and we need to consider the importance of that depletion in these arguments. Assuming that the mass lost from winds is much less than the total mass in the system (Fullerton et al. 2006; Smith 2014), we can estimate the change in angular momentum due to winds as $\Delta J_{\rm wind\ loss} \approx \Delta M_* R_*^2 \omega_*$, and that gained from spin-up as $\Delta J_{\rm spin\ up} \approx M_* R_*^2 \omega_* (\Delta(a)/a)$. The net gain in angular momentum of the star (due to a decrease in orbital separation) is then $\Delta J_* = J_{\rm spin\ up} - J_{\rm wind\ loss}$. The assumption that angular momentum loss due to winds is negligible compared to the gain due to decreasing binary separation and spin-up of the star amounts to the following condition:

$$\frac{\Delta J_{\rm wind\ loss}}{\Delta J_{\rm spin\ up}} \approx \left(\frac{\Delta M}{M} \right) \left(\frac{a}{\Delta a} \right) < 1 \tag{10}$$

or

$$\frac{\Delta a}{a} > \frac{\Delta M}{M}. \tag{11}$$

Falanga et al. (2015) provide estimates of mass loss and observed change in orbital period in the types of binary systems we are considering. From the data in their Tables 1, 3, and 9, we see that the condition in Equation (11) above generally holds—in other words, the fractional change in binary

separation is larger than the fractional mass loss in these systems, and we can invoke Equation (9) going forward. Then, using $T_{\rm dur} \propto J_*^{7/4}$ (Lloyd-Ronning 2022) and Equation (9), we find

$$T_{\rm int} \propto Z^{21\beta/16}. \tag{12}$$

Now consider Z's dependence on redshift. Figure 2 of Fynbo et al. (2006) and Figure 14 of Madau & Dickinson (2014) show how cosmic metallicity increases with decreasing redshift. Although there is ample scatter in the data, we can approximate the relationship roughly as $Z \propto (1 + z)^{-0.4}$. Substituting that relation into Equation (12) leads to

$$T_{\rm int} \propto (1 + z)^{-21\beta/40} \approx (1 + z)^{-0.5\beta} \tag{13}$$

assuming mass loss is roughly proportional to $Z^{1/2}$. For mass loss proportional to $Z^{1/4}$, we find

$$T_{\rm int} \propto (1 + z)^{-21\beta/80} \approx (1 + z)^{-0.25\beta}. \tag{14}$$

As discussed in Section 2, the observed anticorrelation between duration and redshift for the larger GRB sample (that is, not separating into radio-bright and -dark subsamples) is approximately parameterized as $T_{\rm dur} \propto (1 + z)^{-0.8 \pm 0.25}$. We conservatively choose constraints on β within the 2σ error bars and find this implies $1 \lesssim \beta \lesssim 3$ for $\Delta M \propto Z^{1/2}$ and $2 \lesssim \beta \lesssim 6$ for $\Delta M \propto Z^{1/4}$. These two metallicity dependences and our model parameter spaces are shown in the two panels of Figure 3.

5. Discussion and Conclusions

In this paper we have examined scenarios in which the average intrinsic prompt duration of GRBs increases with decreasing redshift, as the data suggest. As metallicity is a variable that we can securely count on increasing over cosmic time (Langeroodi et al. 2022), we have in particular linked this cosmological evolutionary trend to the metallicity of the system. We have considered both single massive stars and massive stars collapsing in interacting binary systems as our GRB progenitors.

Our main results are summarized as follows:

1. Single massive star GRB progenitors may produce the duration–redshift anticorrelation as a result of higher-metallicity stars having larger radii and being able to form more extended accretion disks with lower accretion rates. We present 1D stellar evolution simulations that support this picture. Provided there is enough angular momentum to launch a jet, the more extended stellar radius of a higher-metallicity star can ultimately lead to longer-duration GRB jets at lower redshift.

2. Massive stars in interacting binary systems may produce the duration–redshift anticorrelation through metallicity-dependent mass loss scenarios (as well as metallicity-dependent equations of state) that lead to a decrease in the binary separation for higher-metallicity, low-redshift systems. This can produce a more pronounced spin-up of the massive star and therefore longer-duration GRBs at lower redshifts. Our key assumption, when connecting the binary separation to the angular momentum of the massive star, is that the tidal locking timescale is shorter than other timescales in our system's evolution, so that the binary separation sets the rotation rate of the massive star ($\omega_* = \sqrt{GM_{\rm tot}/a^3}$).
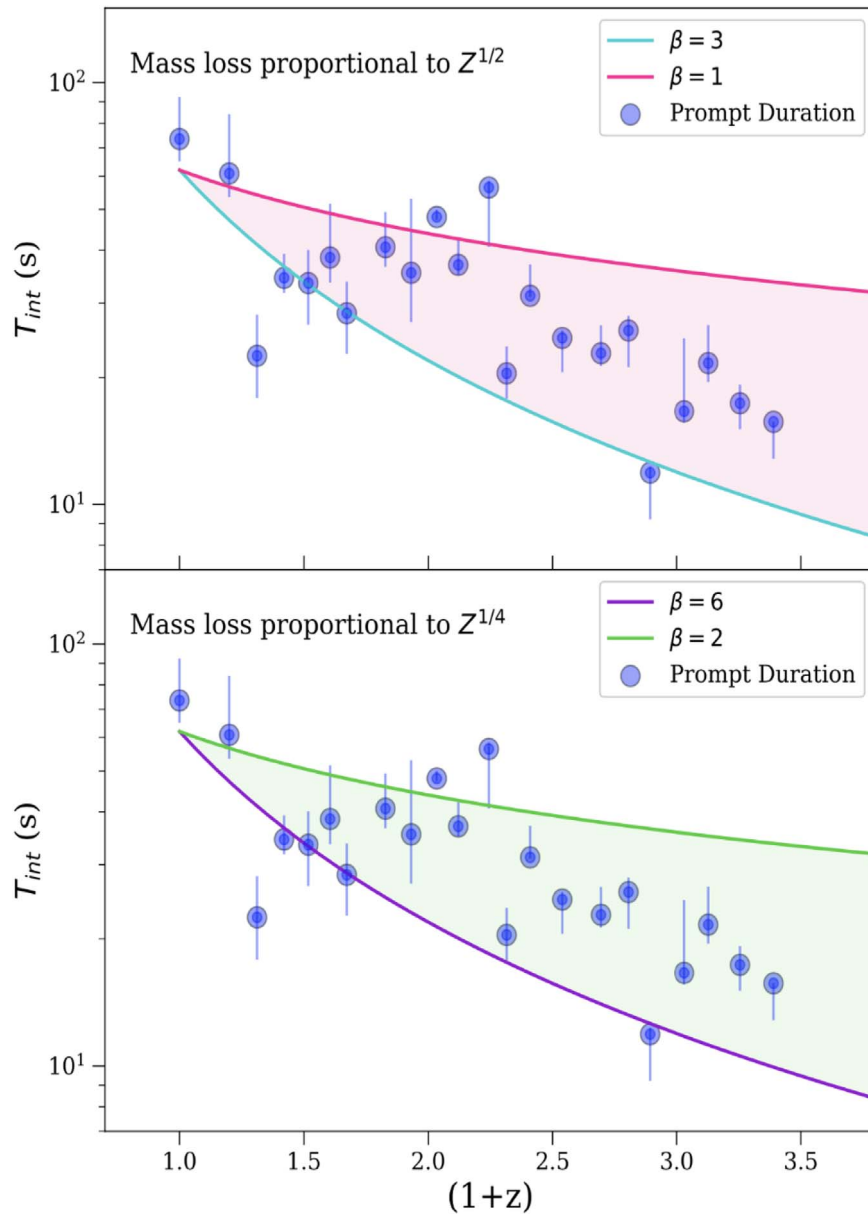
Figure 3. Upper panel: range of β values that accommodate the trend seen in the data, in the context of a massive star collapsing in an interacting binary. The parameter β describes how the binary orbit shrinks as a function of mass loss, where we assume mass loss depends on metallicity to the 1/2 power. Lower panel: same as the upper panel, but here we assume mass loss depends on metallicity to the 1/4 power.

Both our single-star and binary-star pictures have made a number of simplifying assumptions. In our single-star models, we have given relatively general arguments and not focused on details of particular progenitors such as RSGs and BSGs versus WR stars. We do note that Crowther (2007) argues that WR stars are more common at high metallicity, and so further examining the correlation in the context of details of different types of massive stars could further illuminate its nature. We have also made the assumption that the single/isolated star has enough angular momentum to launch a GRB jet. In our binary scenario, we have implicitly assumed that a larger angular momentum reservoir present in the massive star at the end of its life will lead to a more rapidly spinning black hole–disk system (produced upon the star's collapse) and therefore a longer GRB. There are many complicated steps connecting the spin of the massive star at the end of its life to the angular momentum of the black hole–disk system after collapse (Qin et al. 2018).

Going forward, we plan to examine our models through more detailed simulations of these systems, particularly the end-of-life state of massive stars in interacting binaries. We will be able to test the range of values that are valid for our parameter β, while also including effects of the stellar equation of state and the star's expansion. We would also like to further examine the dichotomy between radio-bright and radio-dark GRBs, particularly the conjecture that GRBs with radio afterglows, which have longer prompt gamma-ray duration, are the result of massive stellar collapse in such interacting binary systems (Lloyd-Ronning 2022). As the data improve and we get a better handle on how to divide the radio-bright and -dark subsamples, this and similar correlations may be key to unlocking any fundamental differences in the underlying progenitor systems of GRBs.

We note again that we are only considering black hole–disk central engines, and not magnetar-driven engines for our

GRBs. In GRBs with magnetar central engines, the GRB can be initially powered by accretion onto a newly born neutron star (e.g., Bernardini et al. 2013; Bernardini 2015); extended emission (like a plateau phase) may result from the spin-down power of the magnetar (Zhang & Mészáros 2001). It is not immediately clear whether these systems would be able to produce the anticorrelation between duration and redshift, although many of the arguments we make in this paper may apply to these systems as well.

Finally, evolution of the population statistics of interacting binaries may also explain the duration–redshift anticorrelation. If there exists a larger population of interacting binary systems (of the type we discuss in Section 4 above) at lower redshifts than at high redshifts, this could account for the trend we see in the data. Indeed, Liu et al. (2021) predict there are fewer close binaries at high redshift, although they examine only Population III stars in their study. On the other hand, Moe et al. (2019) and Bate (2019) suggest the close binary fraction is anticorrelated with metallicity. The latter in particular explore the dependence of fragmentation on metallicity and find—for low-mass stars—there is a *higher* close binary fraction at *lower* metallicity (although Kuruwita & Haugbølle 2022, who explore binary separation in situ, suggest disk fragmentation is not a dominant pathway for binaries of close separation). We emphasize that it is not just the interacting binary fraction but the *overall* binary fraction that may depend on metallicity. For example, Neugent (2021) compared the RSG binary fraction in M31 and M33, and showed that it indeed depends on metallicity, with higher-metallicity environments leading to a higher RSG binary fraction (while Moe et al. 2019, for example, again showed the binary fraction for solar-type stars *decreases* with metallicity). Needless to say, this is a complex relation that warrants further examination. A closer look at the viability of this pathway to explain the duration–redshift trend we see in the data requires detailed and informed population synthesis modeling, which we explore in a future paper.

ORCID iDs

Nicole Lloyd-Ronning ⓘ https://orcid.org/0000-0003-1707-7998
Jarrett Johnson ⓘ https://orcid.org/0000-0001-8002-2661
Roseanne M. Cheng ⓘ https://orcid.org/0000-0002-4854-8636

References

Angulo, C., Arnould, M., Rayet, M., et al. 1999, NuPhA, 656, 3
Bate, M. R. 2019, MNRAS, 484, 2341
Bernardini, M. G. 2015, JHEAp, 7, 64
Bernardini, M. G., Campana, S., Ghisellini, G., et al. 2013, ApJ, 775, 67
Blouin, S., Shaffer, N. R., Saumon, D., & Starrett, C. E. 2020, ApJ, 899, 46
Boyajian, T. S., von Braun, K., van Belle, G., et al. 2012, ApJ, 757, 112
Broekgaarden, F. S., Berger, E., Stevenson, S., et al. 2022, MNRAS, 516, 5737
Cassisi, S., Potekhin, A. Y., Pietrinferni, A., Catelan, M., & Salaris, M. 2007, ApJ, 661, 1094
Chakraborty, A., Dainotti, M., Cantrell, O., & Lloyd-Ronning, N. 2023, MNRAS, 520, 5764
Chugunov, A. I., Dewitt, H. E., & Yakovlev, D. G. 2007, PhRvD, 76, 025028
Chun, S.-H., Yoon, S.-C., Jung, M.-K., Kim, D. U., & Kim, J. 2018, ApJ, 853, 79
Crowther, P. A. 2007, ARA&A, 45, 177
Cyburt, R. H., Amthor, A. M., Ferguson, R., et al. 2010, ApJS, 189, 240
Davé, R. 2008, MNRAS, 385, 147
Efron, B., & Petrosian, V. 1992, ApJ, 399, 345
Falanga, M., Bozzo, E., Lutovinov, A., et al. 2015, A&A, 577, A130
Farrell, E., Groh, J. H., Meynet, G., & Eldridge, J. J. 2022, MNRAS, 512, 4116
Ferguson, J. W., Alexander, D. R., Allard, F., et al. 2005, ApJ, 623, 585
Fukushima, H., Omukai, K., & Hosokawa, T. 2018, MNRAS, 473, 4754
Fuller, G. M., Fowler, W. A., & Newman, M. J. 1985, ApJ, 293, 1
Fullerton, A. W., Massa, D. L., & Prinja, R. K. 2006, ApJ, 637, 1025
Fynbo, J. P. U., Starling, R. L. C., Ledoux, C., et al. 2006, A&A, 451, L47
Galama, T. J., Vreeswijk, P. M., van Paradijs, J., et al. 1998, Natur, 395, 670
Georgy, C., Ekström, S., Eggenberger, P., et al. 2013, A&A, 558, A103
Georgy, C., Ekström, S., Meynet, G., et al. 2012, A&A, 542, A29
Georgy, C., Meynet, G., Walder, R., Folini, D., & Maeder, A. 2009, A&A, 502, 611
Gieser, C., Beuther, H., Semenov, D., et al. 2021, A&A, 648, A66
Gladman, B., Quinn, D., Nicholson, P., & Rand, R. 1996, Icar, 122, 166
Halevi, G., Wu, B., Moesta, P., et al. 2022, ApJL, 944, L38
Han, X. H., Hammer, F., Liang, Y. C., et al. 2010, A&A, 514, A24
Harada, R., Onishi, T., Tokuda, K., et al. 2019, PASJ, 71, 44
Heger, A., Fryer, C. L., Woosley, S. E., Langer, N., & Hartmann, D. H. 2003, ApJ, 591, 288
Hjorth, J., & Bloom, J. S. 2012, in Gamma-Ray Bursts, ed. C. Kouveliotou, R. A. M. J. Wijers, & S. Woosley (Cambridge: Cambridge Univ. Press), 169
Hjorth, J., Sollerman, J., Møller, P., et al. 2003, Natur, 423, 847
Houdebine, E. R. 2008, MNRAS, 390, 1081
Huang, Y.-Y., Zhang, H.-M., Yan, K., Liu, R.-Y., & Wang, X.-Y. 2022, ApJL, 940, L36
Iglesias, C. A., & Rogers, F. J. 1993, ApJ, 412, 752
Iglesias, C. A., & Rogers, F. J. 1996, ApJ, 464, 943
Irwin, A. W. 2004, The FreeEOS Code for Calculating the Equation of State for Stellar Interiors, Astrophysics Source Code Library, ascl:1211.002
Janiuk, A., & Proga, D. 2008, ApJ, 675, 519
Jermyn, A. S., Schwab, J., Bauer, E., Timmes, F. X., & Potekhin, A. Y. 2021, ApJ, 913, 72
Kelley, R. L., Rappaport, S., Clark, G. W., & Petro, L. D. 1983, ApJ, 268, 790
Kumar, P., Narayan, R., & Johnson, J. L. 2008a, Sci, 321, 376
Kumar, P., Narayan, R., & Johnson, J. L. 2008b, MNRAS, 388, 1729
Kuruwita, R., & Haugbølle, T. 2022, arXiv:2209.01909
Langanke, K., & Martínez-Pinedo, G. 2000, NuPhA, 673, 481
Langeroodi, D., Hjorth, J., Chen, W., et al. 2022, arXiv:2212.02491
Laskar, T., Berger, E., Chornock, R., et al. 2018a, ApJ, 858, 65
Laskar, T., Berger, E., Margutti, R., et al. 2018b, ApJ, 859, 134
Laskar, T., Berger, E., Tanvir, N., et al. 2014, ApJ, 781, 1
Lee, A., Bloom, E. D., & Petrosian, V. 2000, ApJS, 131, 21
Levine, A., Rappaport, S., Deeter, J. E., Boynton, P. E., & Nagase, F. 1993, ApJ, 410, 328
Levine, A. M., Rappaport, S. A., & Zojcheski, G. 2000, ApJ, 541, 194
Lin, W. L., Wang, X. F., Wang, L. J., & Dai, Z. G. 2020, ApJL, 903, L24
Liu, B., Meynet, G., & Bromm, V. 2021, MNRAS, 501, 643
Liu, T., Song, C.-Y., Zhang, B., Gu, W.-M., & Heger, A. 2018, ApJ, 852, 20
Lloyd-Ronning, N. 2022, ApJ, 928, 104
Lloyd-Ronning, N., Hurtado, V. U., Aykutalp, A., Johnson, J., & Ceccobello, C. 2020, MNRAS, 494, 4371
Lloyd-Ronning, N. M., Aykutalp, A., & Johnson, J. L. 2019a, MNRAS, 488, 5823

Lloyd-Ronning, N. M., Gompertz, B., Pe'er, A., Dainotti, M., & Fruchter, A. 2019b, ApJ, 871, 118
Lü, J., Zou, Y.-C., Lei, W.-H., et al. 2012, ApJ, 751, 49
Lynden-Bell, D. 1971, MNRAS, 155, 95
Maccarone, T. J., Kundu, A., & Zepf, S. E. 2004, ApJ, 606, 430
MacFadyen, A. I., & Woosley, S. E. 1999, ApJ, 524, 262
Madau, P., & Dickinson, M. 2014, ARA&A, 52, 415
Maeder, A. 2002, A&A, 392, 575
Maeder, A., & Meynet, G. 2001, A&A, 373, 555
Meynet, G., & Maeder, A. 2005, A&A, 429, 581
Moe, M., Kratter, K. M., & Badenes, C. 2019, ApJ, 875, 61
Nagakura, H., Suwa, Y., & Ioka, K. 2012, ApJ, 754, 85
Nakauchi, D., Suwa, Y., Sakamoto, T., Kashiyama, K., & Nakamura, T. 2012, ApJ, 759, 128
Neugent, K. F. 2021, ApJ, 908, 87
Oda, T., Hino, M., Muto, K., Takahara, M., & Sato, K. 1994, ADNDT, 56, 231
Olivier, G. M., Lopez, L. A., Auchettl, K., et al. 2022, arXiv:2212.02514
Paxton, B. 2021, Modules for Experiments in Stellar Astrophysics (MESA), r21.12.1, Zenodo, doi:10.5281/zenodo.5798242
Paxton, B., Bildsten, L., Dotter, A., et al. 2011, ApJS, 192, 3
Paxton, B., Cantiello, M., Arras, P., et al. 2013, ApJS, 208, 4
Paxton, B., Marchant, P., Schwab, J., et al. 2015, ApJS, 220, 15
Paxton, B., Schwab, J., Bauer, E. B., et al. 2018, ApJS, 234, 34
Paxton, B., Smolec, R., Schwab, J., et al. 2019, ApJS, 243, 10
Perna, R., Lazzati, D., & Cantiello, M. 2018, ApJ, 859, 48
Postnov, K. A., & Yungelson, L. R. 2014, LRR, 17, 3
Potekhin, A. Y., & Chabrier, G. 2010, CoPP, 50, 82
Poutanen, J. 2017, ApJ, 835, 119
Proga, D., & Begelman, M. C. 2003, ApJ, 592, 767
Puls, J., Vink, J. S., & Najarro, F. 2008, A&ARv, 16, 209
Qin, Y., Fragos, T., Meynet, G., et al. 2018, A&A, 616, A28
Quataert, E., & Kasen, D. 2012, MNRAS, 419, L1
Ramachandran, V. 2022, arXiv:2211.12153
Rogers, F. J., & Nayfonov, A. 2002, ApJ, 576, 1064
Sanyal, D., Langer, N., Szécsi, D., Yoon, S.-C., & Grassitelli, L. 2017, A&A, 597, A71
Saumon, D., Chabrier, G., & van Horn, H. M. 1995, ApJS, 99, 713
Schrøder, S. L., MacLeod, M., Ramirez-Ruiz, E., et al. 2021, arXiv:2107.09675
Smith, N. 2014, ARA&A, 52, 487
Suwa, Y., & Ioka, K. 2011, ApJ, 726, 107
Tauris, T. M., & van den Heuvel, E. P. J. 2006, in Compact Stellar X-ray Sources, ed. W. Lewin & M. van der Klis (Cambridge: Cambridge Univ. Press), 623
Timmes, F. X., & Swesty, F. D. 2000, ApJS, 126, 501
Tout, C. A., Pols, O. R., Eggleton, P. P., & Han, Z. 1996, MNRAS, 281, 257
Toyouchi, D., Hosokawa, T., Sugimura, K., Nakatani, R., & Kuiper, R. 2019, MNRAS, 483, 2031
Vink, J. S., de Koter, A., & Lamers, H. J. G. L. M. 2001, A&A, 369, 574
Wei, Y.-F., & Liu, T. 2022, ApJ, 936, 182
Woosley, S., & Bloom, J. 2006, ARA&A, 44, 507
Woosley, S. E. 1993, ApJ, 405, 273
Woosley, S. E., & Heger, A. 2006, ApJ, 637, 914
Woosley, S. E., & MacFadyen, A. I. 1999, A&AS, 138, 499
Wu, X.-F., Hou, S.-J., & Lei, W.-H. 2013, ApJL, 767, L36
Xin, C., Renzo, M., & Metzger, B. D. 2022, MNRAS, 516, 5816
Yoon, S. C., Langer, N., & Norman, C. 2006, A&A, 460, 199
Zhang, B., & Mészáros, P. 2001, ApJL, 552, L35